Angewandte Chemie
Eine Zeitschrift der Gesellschaft Deutscher Chemiker

Supporting Information

69451 Weinheim, Germany

Fourier Transform EPR Spectroscopy of Trityl Radicals for Multifunctional Assessment of Chemical Microenvironment**

*Andrey A. Bobko, Ilirian Dhimitruka, Jay L. Zweier, and Valery V. Khramtsov**

anie_201310841_sm_miscellaneous_information.pdf

Supporting Information

Table of content

1) Materials and methods **p. S2**

2) FT-EPR spectra simulation **p. S3**

3) Figure SI3 **p. S7**

4) References **p. S8**

Materials and Methods

Synthesis. The monophosphonated trityl probe, p_1TAM (Scheme 1, main manuscript) was synthesized as previously described[1].

pH titration. Radical solutions (200 μM) in the presence of 150 mM of NaCl and various concentration of phosphate buffer were titrated by addition of a small volume of NaOH or HCl with the final dilution of sample less than 1%. Anoxic conditions were maintained using gas controller (Noxygen, Germany) or by addition of 10 mM glucose and glucose oxidase (Sigma, USA, 100 U/ml).

Pulse X-band EPR studies. Measurements were performed on X-band ELEXSYS E 580 EPR spectrometer (Bruker, Germany) at room temperature, 22 °C. Gas composition was controlled by a gas controller (Noxygen, Germany) using teflon tubes with a diameter of 1.14 mm and wall thickness of 60 μm (Zeus, Inc., USA).

T_1 and T_2 relaxation time measurements.

T_2 relaxation times of low-field component of p_1TAM spectrum were measured by using the simple Hahn echo sequence: p0 – tau – p1 – tau – echo. Typical instrument setting were as follows: TWT microwave power, 18 dB; video bandwidth, 20 MHz; time base, 20 ns; 16-step phase cycling; π/2 pulse (p0), 96ns; π pulse (p1), 192 ns; initial tau value, 400 ns, integration time pg, 800 ns. Acquired decay kinetics was fitted by exponent to find a T_2 values.

T_1 relaxation times of low-field component of p_1TAM spectrum were measured by using the inversion recovery pulse sequence (p2 – d2 – p0 – tau – p1 – tau – echo). Typical instrument setting were as follows: TWT microwave power, 18 dB; video bandwidth, 20 MHz; time base, 20 ns; 4-step phase cycling; π/2 pulse (p0), 96ns; π pulse (p1), 192 ns; inversion pulse (p2), 180 ns; initial tau value, 500 ns, d2 delay time, 500 ns; integration time pg, 800 ns. Acquired decay kinetics was fitted by stretched exponent to find a T_1 values.

Fourier Transform EPR signal detection and processing.

EPR signal of p_1TAM probe was acquired in the form of free induction decay (FID) using two different settings: (i) non-selective 20 ns π/2 pulse for allowing for excitation of the whole spectrum, and (ii) selective 96 ns π/2 pulse for selective excitation of low-field spectral component. Typical instrument setting were as follows: TWT microwave power, 18 dB (96 ns pulse) or 3 dB (20 ns pulse); video bandwidth, 20 MHz. Signal acquisition parameters: detection time, 4096 points x 20 ns time base = 81.92 μs; number of transient averages, a = 500; phase cycling, 4-step phase cycle; number of averages, n = 20.

Acquired FID signal was reconstructed to remove dead-time gap using linear prediction fitting program embedded in X-Epr software (Bruker, Germany). The resulted FIDs were zero-filled up to 16384 points, FT-processed, baseline- and phase-corrected.

FT-EPR spectra simulation.

Simulation of spectra acquired with non-selective 20 ns π/2 pulse microwave pulse.

Whole FT EPR spectrum of p_1TAM obtained after non-selective π/2 pulse is characterized by a doublet for p_1TAM^{3-} form (for pH below dissociation constant of phosphono group, pH<<pK_a) and p_1TAM^{4-} form (pH>> pK_a) or by quartet at pH~pK_a when both ionization states are present (see Fig. 1, main manuscript). These spectra were simulated using theory of exchange between several sites in non-coupled or loosely coupled systems, adopted from ref.[2]. Briefly, FT EPR absorption signal V was described as follows:

$$V(\nu) = \mathrm{Re}\mathbf{1}\mathbf{K}^{-1}\mathbf{P} \quad (1)$$

$$\mathbf{K} = \mathbf{D} - \mathbf{R} - i(\mathbf{\Omega} - \nu\mathbf{I}) \quad (2)$$

where

$$\mathbf{1} = \begin{pmatrix} 1 \\ 1 \\ 1 \\ 1 \end{pmatrix}; \quad \mathbf{P} = \begin{pmatrix} p_A \\ p_B \\ p_B \\ p_A \end{pmatrix}; \quad \mathbf{I} = \begin{pmatrix} 1 & 0 & 0 & 0 \\ 0 & 1 & 0 & 0 \\ 0 & 0 & 1 & 0 \\ 0 & 0 & 0 & 1 \end{pmatrix}; \quad \mathbf{\Omega} = \begin{pmatrix} \nu_1 & 0 & 0 & 0 \\ 0 & \nu_2 & 0 & 0 \\ 0 & 0 & \nu_3 & 0 \\ 0 & 0 & 0 & \nu_4 \end{pmatrix};$$

$$\mathbf{R} = \begin{pmatrix} 1/T_A + R_{O_2}^A & 0 & 0 & 0 \\ 0 & 1/T_B + R_{O_2}^B & 0 & 0 \\ 0 & 0 & 1/T_B + R_{O_2}^B & 0 \\ 0 & 0 & 0 & 1/T_A + R_{O_2}^A \end{pmatrix}; \quad \mathbf{D} = \begin{pmatrix} r_1 & r_{21} & r_{31} & r_{41} \\ r_{12} & r_2 & r_{32} & r_{42} \\ r_{13} & r_{23} & r_3 & r_{43} \\ r_{14} & r_{24} & r_{34} & r_4 \end{pmatrix}$$

where p_A and p_B=(1-p_A) – fraction of p_1TAM^{3-} and p_1TAM^{4-} forms of p_1TAM probe, correspondingly; ν_1-ν_4 are the frequencies of four observed EPR lines, namely, $\nu_1 = -0.5\times a_P(A) + \nu_0$, where a_P is phosphorus hyperfine splitting constant for p_1TAM^{3-} ionization state of p_1TAM probe (in Hz) and ν_0 is frequency offset; ν_2=$-0.5\times a_P(B)+\nu_0-\Delta g$, where Δg is difference between resonance positions of p_1TAM^{3-} and p_1TAM^{4-} forms (in Hz) due to corresponding difference in g-factors; ν_3=$0.5\times a_P(B)+\nu_0-\Delta g$, ν_4 =$0.5\times a_P(A)+\nu_0$; T_A and T_B are transverse relaxation times of p_1TAM^{3-} and p_1TAM^{4-} forms, correspondingly; $R_{O_2}^A$ and $R_{O_2}^B$ are the rates of oxygen-induced relaxation (in Hz) for p_1TAM^{3-} and p_1TAM^{4-} forms, correspondingly. **D** represents frequency exchange matrix where r_{ij} is the rate of frequency exchange (in Hz) between spectral line i and j (i, j=1, 2, 3, 4) where $r_1 = r_{11} + r_{12} + r_{13} + r_{14}$, $r_2 = r_{21} + r_{22} + r_{23} + r_{24}$, $r_3 = r_{31} + r_{32} + r_{33} + r_{34}$, $r_4 = r_{41} + r_{42} + r_{43} + r_{44}$. Figure SI1 schematically shows p_1TAM EPR spectral pattern and various chemical exchange processes that contribute to the values of r_{ij}.

.

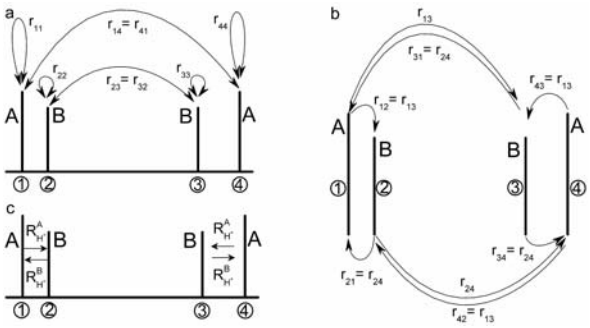

Figure SI1. The schematic illustration of p_1TAM EPR spectral pattern and various chemical exchange processes that affect the widths and positions of spectral lines: (**a**) spin exchange between the p_1TAM molecules in the same ionization states, A or B; (**b**) spin exchange between the p_1TAM molecules in different ionization states; (**c**) proton exchange between the states A and B.

Both spin exchange and proton exchange reactions contribute to the frequency exchange between the lines with the same phosphorus nucleus spin projections, 1↔2 and 3↔4. The exchange rates between the other lines are determined by the spin exchange only as shown in Figure 7a and 7b, namely:

$$r_{11} = r_{14} = r_{41} = r_{44} = k_{AA}\times p_A\times[p_1TAM] \quad (3)$$

$$r_{22} = r_{23} = r_{32} = r_{33} = k_{BB}\times(1-p_A)\times[p_1TAM] \quad (4)$$

$$r_{13} = r_{42} = k_{AB}\times(1-p_A)\times[p_1TAM] \quad (5)$$

$$r_{24} = r_{31} = k_{AB}\times p_A\times[p_1TAM] \quad (6)$$

where k_{AA}, k_{BB} and k_{AB} are the bimolecular rate constants for the spin exchange reaction between the radicals in the same ionization state, p_1TAM^{3-} (k_{AA}) or p_1TAM^{4-} (k_{BB}), or between the radicals in different ionization states, p_1TAM^{3-} and p_1TAM^{4-} (k_{AB}).

The four other frequency exchange rates, r_{12}, r_{21}, r_{34} and r_{43}, are determined by both spin exchange and proton exchange reactions, namely:

$$r_{12} = r_{43} = r_{13}+R^A_{H+} = k_{AB}\times(1-p_A)\times[p_1TAM] + R^A_{H+} \quad (7)$$

$$r_{21} = r_{34} = r_{24}+ R^B_{H+} = k_{AB}\times p_A\times[p_1TAM]+ R^A_{H+}\times p_A/(1-p_A) \quad (8)$$

where R^A_{H+} is the rate of proton loss by phosphono group of p_1TAM^{3-} form and R^B_{H+} is the rate of proton addition to phosphono group of p_1TAM^{4-} form. The ratio R^A_{H+}/ R^B_{H+} is equal to the ratio of inverse lifetimes of the radical in these forms or the fraction ratio, so $R^B_{H+}= R^A_{H+}\times p_A/(1-p_A)$. These proton exchange rates may be enhanced in the presence of buffer molecules.

The convolution of function V(ν) with Gaussian function was used to take into account the unresolved super hyperfine structure in the EPR spectra of p_1TAM probe:

$$F(\nu) = C + D\cdot\int V(x)\cdot e^{\frac{-2\cdot(\nu-x)^2}{G^2}}\cdot\frac{\sqrt{2}}{\sqrt{\pi}\cdot G}dx \quad (9)$$

where C and D are numerical coefficients; G is linewidth of Gaussian distribution. In general case the spectrum shape, F(ν), is determined by all the discussed parameters: C, D, p_A, $a_P(A)$, $a_P(B)$, Δg, T_A, T_B, G, Ro_2^A, Ro_2^B, $k_{AA}^*=k_{AA}\times[p_1TAM]$, $k_{BB}^*=k_{BB}\times[p_1TAM]$, $k_{AB}^*=k_{AB}\times[p_1TAM]$, R^A_{H+}. In order to decrease a number of variables, the intrinsic spectral parameters, $a_P(p_1TAM^{3-})$, $a_P(p_1TAM^{4-})$, Δg, T_A, T_B, and G were first determined by least-squares fitting of the function F(ν) to experimental FT EPR spectra in anoxic solutions at low radical and buffer concentrations when spin and proton exchange contributions are negligible, i.e. Ro_2^A, Ro_2^B, k_{AA}^*, k_{BB}^*, k_{AB}^*, $R^A_{H+}<<1/T_A$, $1/T_B$. The fitting FT EPR spectra of anoxic 150 mM NaCl solution of 50 μM p_1TAM by eq. (1) yields the values $a_P(p_1TAM^{3-})$=10191 kHz, $1/T_A$ = 46 kHz and G_A=85 kHz for the spectrum acquired at pH 4.5; and $a_P(p_1TAM^{4-})$ =9422 kHz, $1/T_B$=32 kHz and G_B=94 kHz for the spectrum acquired at pH 11.0. For the spectra acquired at intermediate value of pH=6.9, when both ionization states of the radical are observed in the spectra, an average value of G (89 kHz) has been fixed during the spectra fitting yielding Δg =90 kHz, $1/T_A$ = 44 kHz, $1/T_B$ = 35 kHz. These parameters have been used in all further calibrations of the spectra sensitivity to oxygen, probe and buffer concentrations.

Determination of bimolecular rate constants of spin self-exchange for p_1TAM probe.

Least-square fitting of FT-EPR spectra of p_1TAM at concentration 0.1-2 mM by eq. (9) was performed using the fixed values of intrinsic spectral parameters pre-determined at low probe concentration as discussed above. The fitting yields the values of k_{AA}^*, k_{BB}^* and k_{AB}^* which show linear dependence on p_1TAM concentration (see Fig. SI2). The determined bimolecular rate constants, k_{AA}=14.3 kHz/mM=1.43×10^7 $M^{-1}s^{-1}$, k_{BB}=7.4 kHz/mM=0.74×10^7 $M^{-1}s^{-1}$, and k_{AB}=10 kHz/mM=10^7 $M^{-1}s^{-1}$, are about three orders of magnitude lower than the rate constants for the diffusion-controlled reaction which is expected for sterically-hindered trityl radicals.

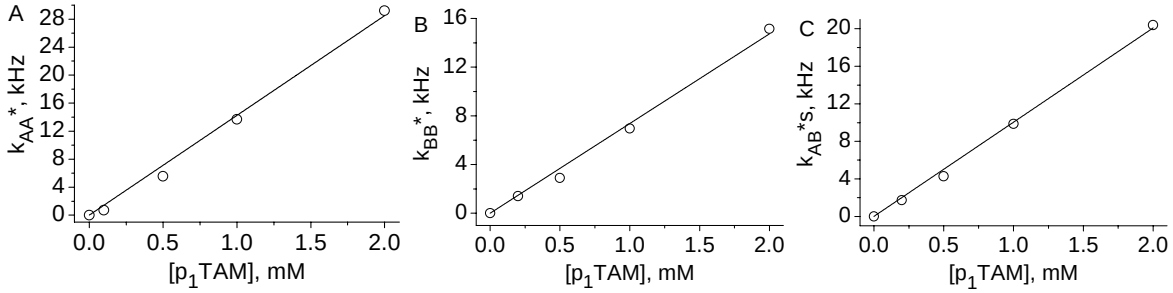

Figure SI2. A. The concentration dependencies of the observed rates of spin self-exchange, k_{AA}^*, k_{BB}^* and k_{AB}^* calculated from the spectra measured in 150 mM NaCl aqueous solutions of p_1TAM at pH 4.5 (**A**), 11.0 (**B**) and 6.9 (**C**). The spectra simulations were performed using $1/T_A$=44 kHz, $1/T_B$=35 kHz and G=89 kHz. The linear fits yield the values of k_{AA}=14.3 kHz/mM; k_{BB}=7.4 kHz/mM, and k_{AB}=10 kHz/mM.

Determination of bimolecular rate constants of proton exchange of p_1TAM probe with phosphate.

The reaction of proton exchange between phosphate buffer and p_1TAM probe can be expressed by following equation:

$$p_1TAM^{3-} + HPO_4^{2-} \underset{k_r}{\overset{k_f}{\rightleftharpoons}} p_1TAM^{4-} + H_2PO_4^- \qquad (10)$$

The rate of proton loss by p_1TAM^{3-} due to the proton transfer to HPO_4^{2-} equals to

$$R_{H+}^A = k_f \cdot [HPO_4^{2-}] = k_f \cdot B_0 \cdot \frac{K_a^B}{H^+ + K_a^B} = k_f \cdot B_0 / \left(\frac{K_a^R}{K_a^B} \cdot \frac{p_A}{1 - p_A} + 1 \right) \qquad (11)$$

Where B_o is a total concentration of phosphate buffer, K_a^B and K_a^R are ionization constants for inorganic phosphate and phosphono group of p_1TAM, correspondingly. Therefore the rate constant k_f can be found by linear approximation of dependence of R_{H+}^A on buffer concentration, B_0, measured at fixed pH value. The value of k_r can be calculated from k_f according to the following equation:

$$k_r = k_f \cdot \frac{[p_1TAM^{3-}] \cdot [HPO_4^{2-}]}{[p_1TAM^{4-}] \cdot [H_2PO_4^-]} = k_f \cdot \frac{K_a^B}{K_a^R} \qquad (12)$$

that provides simple relationship, $k_r = 1.55 \times k_f$, for aqueous solutions with ionic strength 0.15 (150 mM NaCl) and temperature 22 °C ($pK_a^B = 6.66$ [3] and $pK_a^R = 6.85$ [1], see Fig.3a, main manuscript). Fitting the EPR spectra of p_1TAM (200 μM) at different concentrations of phosphate buffer and fixed pH value close to pK_a^R using the values of $1/T_A$ = 44 kHz, $1/T_B$ = 35 kHz, G = 89 kHz, k_{AA} = 14.3 kHz/mM, k_{BB} = 7.2 kHz/mM and k_{AB} = 10 kHz/mM yields corresponding R_{H+}^A values. The linear approximation of R_{H+}^A dependence on phosphate concentration (Fig. 6a, main manuscript) in the range from 0 to 20 mM allows for calculation of bimolecular rate constants, k_f=21 kHz/mM=2.1×10^7 $M^{-1}s^{-1}$ and k_r =33 kHz/mM=3.3×10^7 $M^{-1}s^{-1}$. At high phosphate buffer concentration (Fig. 4, main manuscript) proton exchange results in fast frequency exchange-induced line narrowing. At 90 mM phosphate, simulation of exchange-narrowed line still allows for evaluation of bimolecular rate constant, $k_f \approx 25$ kHz/mM. The obtained values of $k_f = 2.1 \times 10^7$ $M^{-1}s^{-1}$ and $k_r = 3.3 \times 10^7$ $M^{-1}s^{-1}$ are 2-3 fold higher than corresponding values of spin self-exchange between ionization states of the trityl probe, k_{AA}, k_{BB} and k_{AB}, which might reflect a difference in the sizes of the large trityl and comparatively small phosphate molecules.

Simulation of spectra acquired with selective microwave pulse.

In case of selective 96 ns π/2 pulse only the part of FT-EPR spectrum of p_1TAM, low-field component of the doublet arisen from phosphorus hyperfine splitting, was acquired. The FT-EPR spectra were simulated as described above, but only low-field part were fitted to the

experimental spectra. First, FT-EPR spectra of anoxic solution of 50 μM p_1TAM were used to determine Lorentzian ($1/T_A$ and $1/T_B$) and Gaussian (G_A and G_B) linewidths. The obtained values, $1/T_A$=46 kHz and $1/T_B$=32 kHz coincide within experimental error with the corresponding values measured using non-selective 96 ns π/2 pulse. The obtained values of G_A=72 kHz and G_B=85 kHz were slightly lower than corresponding values measured using non-selective pulse. In the following simulations of the FT spectra obtained using selective pulse, an average value of G (79 kHz) was used.

Determination of the rate constants of spin exchange of p_1TAM with oxygen.

FT-EPR spectra were acquired using selective pulse experiment mode at different oxygen partial tensions and three pH values: pH 11 (pH>>pK_a), pH 4.5 (pH<<pK_a) and pH 6.9 (pH≈pK_a). Least-square fitting of FT-EPR spectra using $1/T_A$=46 kHz, $1/T_B$=32 kHz and G=79 kHz yield the values of oxygen-induced relaxation rates, $R_{O_2}^A$ and $R_{O_2}^B$. The linear fitting of the dependencies of $R_{O_2}^A$ and $R_{O_2}^B$ on oxygen partial pressure yields the corresponding bimolecular rate constants, $k_{O_2}^A$ =1.51 kHz/mmHg and $k_{O_2}^B$ =1.38 kHz/mmHg (see Figure 3b, manuscript). Supposing oxygen solubility in aqueous solution with 150 mM NaCl at 22 °C and pO_2=760 mmHg, ≈1.28 mM, we get the values of $k_{O_2}^A$ =0.9×10^9 M^{-1}s^{-1} and $k_{O_2}^B$ =0.82×10^9 M^{-1}s^{-1} being close to rate constants for diffusion-controlled reactions.

FT-EPR spectra of p1TAM probe solutions of different compositions

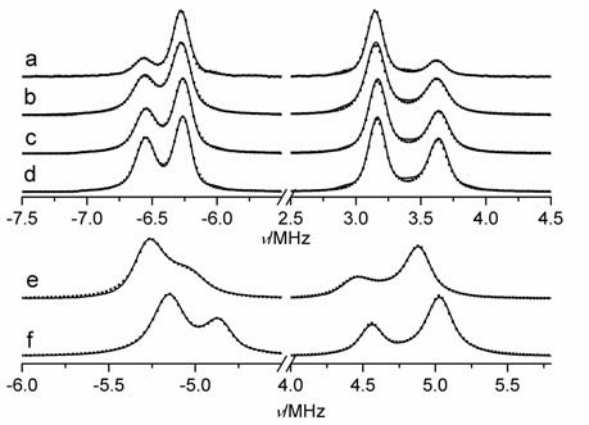

Figure SI3. FT-EPR spectra of p_1TAM probe solutions of different composition shown in Table 2 (the order of the spectra from a to f corresponds to the order of rows from top to bottom in the Table 2). The dotted lines represent the best fit of the calculated spectra yielding the parameters of pH, pO_2 and concentrations of phosphate and p_1TAM shown in Table 2 (main manuscript).

References:

[1] I. Dhimitruka, A. A. Bobko, T. D. Eubank, D. A. Komarov, V. V. Khramtsov, *JACS* **2013**, *135*, 5904−5910.

[2] M. L. Martin, G. J. Martin, J.-J. Delpuech, *Practical NMR spectroscopy*, Heyden, London; Philadelphia, **1980**.

[3] J. N. Butler, *Ionic equilibrium: solubility and pH calculations*, Wiley, New York, **1998**.